Environmental Nanotechnology, Monitoring & Management 12 (2019) 100260

Contents lists available at ScienceDirect

Environmental Nanotechnology, Monitoring & Management

journal homepage: www.elsevier.com/locate/enmm

Nanocrystalline cellulose from waste paper: Adsorbent for azo dyes removal

Jindrayani Nyoo Putro[a], Shella Permatasari Santoso[b], Felycia Edi Soetaredjo[b], Suryadi Ismadji[b,*], Yi-Hsu Ju[a,*]

[a] Department of Chemical Engineering, National Taiwan University of Science and Technology, No. 43, Sec 4, Keelung Rd,. Da'an District, Taipei City, 10607, Taiwan
[b] Department of Chemical Engineering, Widya Mandala Surabaya Catholic University, Kalijudan 37, Surabaya, 60114, Indonesia

ARTICLE INFO

Keywords:
Nanocellulose
Waste paper
Isotherms
Adsorption
Azo dyes

ABSTRACT

The preparation of nanocrystalline cellulose from waste printed papers as adsorbent was conducted using organic solvent. The synthesize of nanocrystalline cellulose is characterized by Fourier transform-infra red (FTIR), scanning electron microscopy (SEM), and transmission electron microscopy (TEM). Hydroxynaphtol blue and congo red in aqueous solutions are used as sorbate in this study to test the single system adsorption capacity of nanocrystalline cellulose using Langmuir and Freundlich isotherm models at 30, 40, and 50 °C. Kinetic study are quantified using pseudo-first order and pesudo-second order models. The adsorption of both azo dyes resulted in negative value of ΔG° which shows spontaneous adsorption of both azo dyes onto adsorbent active sites. Higher temperature increase the adsorption of dyes represents the endothermic nature of adsorption and randomness of adsorbent-solution interface.

1. Introduction

One of the causes of water shortage in earth is due to increased pollution. Textile industry is one of the largest contributor of water pollution, the World Bank estimates 20% of global industrial wastewater comes from the treatment and dyeing of textiles (Kant, 2012a,b). Exposure of dye wastewater can harm human health and living organism ecosystem, thus removal of dye wastewater is needed. For many decades, the utilization of natural adsorbent has attracted many researcher around the world due to their abundance, easy modification, and high adsorption performance (Crini, 2006a,b; Gupta and Suhas, 2009a,b). Nanocrystalline cellulose (NCC) has been used as adsorbents for many wastewater treatment, such as heavy metal and dye (He et al., 2013a,b; Yu et al., 2013a,b). This crystalline part can be extracted from cellulose fibrils which usually has length of 50–150 nm (Ioelovich, 2008a,b). The simplest method to obtain NCC is using the acid hydrolysis under certain acid concentration and temperature. Due to its hydroxymethyl functional groups, NCC can be versatily modified with other chemicals to enhance its adsorption capacity. Some reports on the removal of anionic and cationic dye using nanocrystalline cellulose (NCC) also gives good performance (Jin et al., 2015a,b; Qiao et al., 2015a,b).

The world produces more than 300 milion tons of paper annually, the consumption of paper is even predicted to be doubled before 2030 (Research Conservation Alliance, 2016). 42% of global wood is used to make papers, causing environmental problems. In the United States, 40% of municipal solid waste comprised of papers and paperboards. In the present study, NCC will be obtained through recycling waste printed paper. Since waste printed paper contains mostly of cellulose, it can be pretreated to remove the toner and hydrolize to produce NCC. The aim of this study is to investigate the feasibility to produce NCC from waste printed paper and the adsorption mechanism of NCC on the removal of azo dye. The adsorption isotherm is studied with Langmuir and Freundlich model, while the kinetic study is determined by pseudo-first and pseudo-second order.

2. Material and method

2.1. Materials

Waste printing paper was obtained from personal laboratory use, the ink type used was toner from HP LaserJet Q7553A. Reagent grade NaOH, HCl, KNO_3, hydroxynaphtol blue, congo red, chloroform, dimethyl sulfoxide, sulfuric acid were used without further purification.

2.2. Pretreatment of waste printed paper to NCC

5 g waste paper was soaked in tap water overnight and shredded using blender. The shredded paper was then deinked with 100 ml organic solvent that consisted of 30% vol. chloroform (99% purity) and

* Corresponding authors.
E-mail addresses: suryadiismadji@yahoo.com (S. Ismadji), yhju@mail.ntust.edu.tw (Y.-H. Ju).

https://doi.org/10.1016/j.enmm.2019.100260
Received 8 July 2019; Received in revised form 16 August 2019; Accepted 3 October 2019

70% vol. dimethyl sulfoxide (99.7% purity). Deinking was done under continuous stirring for 2 h at room temperature. After that, the solution was sonicated for 15 min, and the waste paper was filtered and rubbed against filter screen to remove the toner. Then waste paper was dried in oven for overnight and kept in desiccator for further usage. Deinked waste paper was dissolved in 1 M NaOH with 10% solid to liquid consistency in order to remove impurities and swell the cellulose fiber. The solution was stirred for 3 h at room temperature and dried in oven at 50 °C for 6 h. Then 1 *g* waste paper was treated with 20 ml of 64% wt. H_2SO_4 at 45 °C for 60 min under continuous stirring. After hydrolysis, the solid and liquid was separated with centrifugation (9503 *g*; 10 min). The centrifuge was done repeatedly until the supernatant became turbid. The turbid supernatant was collected and posed in dialysis tube with 12–14 kDa molecular weight cut off for 3 days. The suspension was sonicated for 30 min in ice water bath to avoid overheating and kept in −20 °C refrigerator for 24 h to freeze dry and obtain the NCC powder.

2.3. Characterization

Scanning electron microscope (SEM) was obtained with JEOL JSM-6500 F to know the surface morphology of samples. Prior to SEM imaging, the samples were coated with thin layer platinum by auto fine coater (JFC-1600, JEOL, Ltd., Japan) for 90 s in an argon atmosphere. The SEM analysis was conudcted at 10 kV with 10.4 mm working distance. Transmission electron microscope (TEM) was conducted to know the NCC morphology by using Tecnai F20 G2 FEI-TEM at 80 kV, the sample was prepared on a 300 mesh Cu grids with 2% uranyl acetate for staining. The attenuated total reflectance (ATR) FTIR analysis was conducted in FTIR Bio-Rad Model FTS-3500. The analysis was operated in frequency range 4000-650 cm^{-1} with 4 cm^{-1} scanning resolution and the signal was accumulated from 100 scans.

2.4. Adsorption experiment

The adsorption of hydroxynapthol blue (HB) and congo red (CR) was conducted in batch mode. Stock solution of HB and CR were prepared by dissolving 100 mg of HB or CR into a liter of distilled water. The adsorption experiments were conducted by introducing various mass of NCC into a series of conical flasks containing 100 ml of HB or CR aqueous solution with a certain pH value. The pH was previously determined by adding 0.1 M HCl or NaOH solution into the solution. The effect of temperature on adsorption isotherm was studied by carrying out the adsorption at different temperature (30, 40 and 50 °C). After equilibrium condition was reached, the solution was separated from the adsorbent by centrifugation at 10,000 rpm for 10 min. The final concentration of HB and CR was measured using Spectrophotometer UV-VIS at λ_{max} = 573 and 497 nm, respectively. Adsorbed HB and CR at equilibrium condition per unit mass of adsorbent (q_e) was calculated by the following equation:

$$q_e = \frac{C_o - C_e}{m} V \quad (1)$$

Where q_e is the equilibrium capacity of HB or CR on the adsorbent (mmol/g), C_o and C_e are the intial and equilibrium concentrations (mmol/L). V is the volume of solution (L), and m is the mass of adsorbent (g).

3. Results and discussion

3.1. Preparation and characterization of adsorbent

After the acid hydrolysis of waste printed paper, NCC will be produced. For each gram of pretreated waste paper hydrolysis resulted in 0.3 g of NCC. Therefore only 30% part of the preteated waste paper can be converted into crystalline cellulose. From the functional group

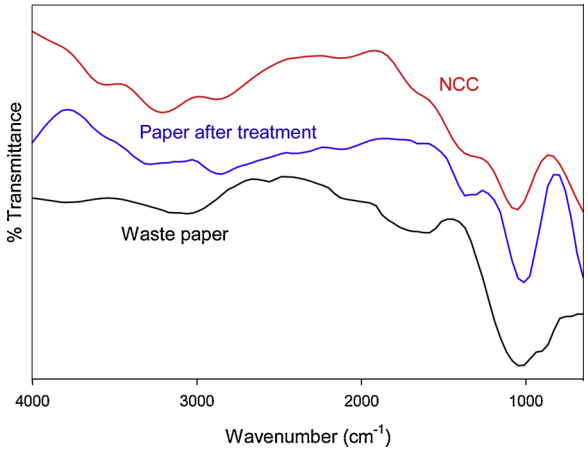

Fig. 1. FTIR result of waste paper, paper after treatment and NCC.

qualification obtained from FTIR, the toner removal was succeeded and the attachment of sulfonate functional group is due to the sulfuric acid hydrolysis. The Fig. 1 represents the spectra of the waste paper, deinked waste paper, and NCC. For waste paper and deinked waste paper, both showed the cellulose characteristics peaks at wavenumber 1024, 1357, 2841 cm^{-1} which correspond to C–O/C-C stretching, C–H bonding, and CH_2 symmetrical stretching, respectively (Garside and Wyeth, 2006; Higgins et al., 1961a, 1961b). The disappearance of peak at 1730 cm^{-1} in deinked waste paper confirm that the removal of toner is succeeded, since that peak conforms the carbonyl band of styrene acrylate copolymer (Lee et al., 2014a, 2014b; Merrill et al., 2003a, 2003b). Following the removal of toner, −OH group show up at 3291 cm^{-1} in deinked waste paper which is expected from the deinking process using organic solvents (Higgins et al., 1961a, 1961b). The spectra of NCC is completely the the same with the waste paper after treatment, but there is spectra swifting appears in the wavenumber 1024 cm^{-1} to 1035 cm^{-1} which indicates the sulfonate functional groups attached to NCC (Lin and Dufresne, 2014a, 2014b).

The surface morphology of waste paper reveals the toner particle on the cellulose surface, as shown in Fig. 2a. After deinking process and alkaline pretreatment, there is no toner on the surface that previously indicated with FTIR result (Fig. 1) and the fiber seems to be loosen up due to NaOH pretreatment (Fig. 2b). After acid hydrolysis, the crystalline nanocellulose was obtained, it can be seen from Fig. 2c the crystal morphology of crystalline cellulose with length distribution of crystal around 271 nm.

3.2. Effect of pH

Adsorption behavior of azo dye is greatly depended on pH, especially it can affect the ionization of the dye. Azo dye has very specific characteristic in certain pH, usually it undergoes protonation in acid condition. The adsorption of HB and CR was optimum in acid condition, 2 and 3, respectively as shown in Fig. 3. The pH 2 was not discussed in the adsorption of congo red due to the aggregation of dye. Usually solvent with high dissociation constant value (D water = 78) will not produce such aggregation (Mera and Davies, 1984a, 1984b). However, water promotes the interaction of dye ion-counter ion interactions thus aggregation occurred in the very low pH condition (McKay and Hillson, 1965a, 1965b). It was clear that NCC exhibits negative surface charge throughout all pH conditions and protonated form of dyes in the low pH attracted each other in this adsorption mechanism. HB is highly protonated in pH 2, since the pKa_1 value of HB is 6.44. As for CR, it can undergo two different protonated (ammonium and azonium) forms, both present in a tautomeric equilibrium mixture (Pigorsch et al., 1994a, 1994b). Adsorption of HB on NCC is certainly higher than CR, because of the dissociation of phenolic hydroxl groups in ortho- and

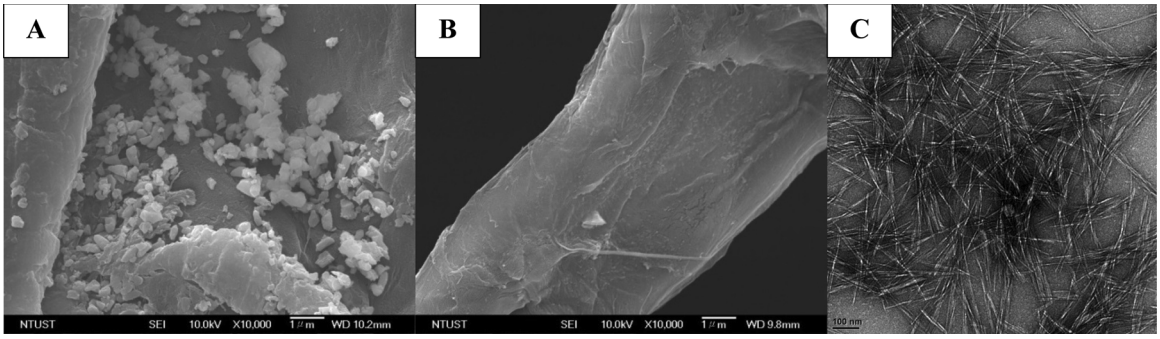

Fig. 2. Morphological image of (A) waste paper, (B) paper after treatment, (C) NCC.

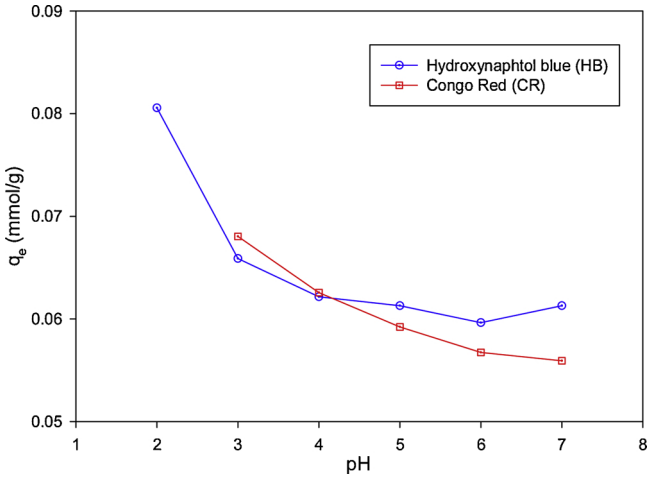

Fig. 3. Effect of pH on the adsorption of azo dyes.

orthó- positions relative to the azo group (Itoh and Ueno, 1970a, 1970b). This protonated −OH has better attractive forces with sulfonate anions in the NCC surface than protonated ammonium or azonium forms of CR. Optimum pH of adsorption CR is 3, where CR is presented in protonated form since the pKa value is 4.1 (Sabnis, 2010a, 2010b).

3.3. Adsorption kinetics

Two well-known models are used to study the adsorption kinetics of azo dye on NCC, they are pseudo-first order and pseudo-second order. Pseudo-first order was first introduced by Lagergren (1898)a, 1898b has mathematical expression as follows

$$q_t = q_e(1 - \exp(-k_1 t)) \quad (1)$$

and the pseudo-second order was later presented by Blanchard et al. (1984)a, 1984b is written as

$$q_t = \frac{q_e^2 k_2 t}{1 + q_e k_2 t} \quad (2)$$

where q_t(mmol/g)andq_e(mmol/g) are the amount of dye adsorbed at equilibrium and at time t (min), respectively. k_1(min^{-1})andk_2(g mmol^{-1}min^{-1}) are the rate constant for pseudo-first and pseudo-second order model, respectively.

The fitting of experimental kinetic data is plotted in Fig. 4, it can be seen that the data was well fitted by both pseudo-first and pseudo-second order. The parameter of models are given in Table 1. Both models give satisfactory fitting towards experimental data based on the correlation factor, however it is clear that other value of parameters from each models have to be taken account into consideration of determining which model gives the best fit. Model fitting HB dye gives interesting results, since it is clear that pseudo-first order gives best

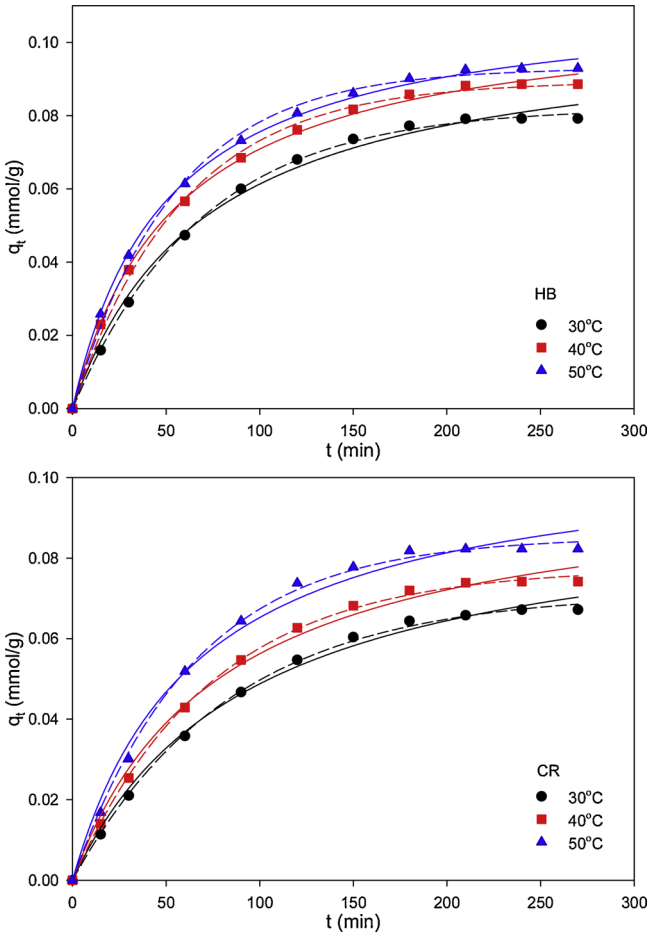

Fig. 4. Adsorption kinetic of azo dyes onto NCC (dashed line: pseudo-first and solid line: pseudo-second).

fitting at all condition, while the value of R^2 from pseudo-second order fitting is a little bit higher than pseudo-first order. It seems that pseudo-second order cannot really described well the equilibrium adsorption of HB, which make it overestimate the value of q_e in all temperature. The adsorption of CR is also following pseudo-first order well with the value of q_e slightly higher than the experimental.

3.4. Adsorption isotherms

Equilibrium profile of dyes adsorption on NCC is studied by two famous models, Langmuir and Freundlich. Two models are capable to describe the interaction of adsorbate and adsorbent throughout the system by using simple two parameters empirical equations. Langmuir has the following form

Table 1
Kinetic parameters for adsorption of azo dyes on NCC at three different temperatures.

Azo dyes	Models	Parameters	Temperature (°C)		
			30	40	50
HB	Pseudo-first order	$q_{e,exp}$(mmol/g)	0.0792	0.0886	0.0929
		k_1(min^{-1})	0.0146	0.0171	0.0184
		$q_{e,cal}$(mmol/g)	0.0822	0.0894	0.0930
		R^2	0.9994	0.9977	0.9969
	Pseudo-second order	$q_{e,exp}$(mmol/g)	0.0792	0.0886	0.0929
		k_2(g mmol^{-1}min^{-1})	0.1345	0.1643	0.1780
		$q_{e,cal}$(mmol/g)	0.1048	0.1101	0.1131
		R^2	0.9944	0.9983	0.9986
CR	Pseudo-first order	$q_{e,exp}$(mmol/g)	0.0672	0.0742	0.0823
		k_1(min^{-1})	0.0119	0.0136	0.0156
		$q_{e,cal}$(mmol/g)	0.0715	0.0776	0.0854
		R^2	0.9991	0.9993	0.9984
	Pseudo-second order	$q_{e,exp}$(mmol/g)	0.0672	0.0742	0.0823
		k_2(g mmol^{-1}min^{-1})	0.1111	0.1267	0.1419
		$q_{e,cal}$(mmol/g)	0.0950	0.1005	0.1079
		R^2	0.9950	0.9943	0.9903

$$q_e = \frac{q_m K_L C_e}{1 + K_L C_e} \quad (1)$$

where q_m is the maximum adsorption capacity (mmol/g) and K_L is the affinity constant (L/mmol). Langmuir also has dimensionless constant called equilibrium parameter which can be expressed as R_L,

$$R_L = \frac{1}{1 + K_L C_o} \quad (2)$$

The value of R_L plays important to determine favorable adsorption in the system. It can indicates specific nature of adsorption to be unfavorable ($R_L > 1$), linear ($R_L = 1$), favorable ($0 < R_L < 1$). Langmuir isotherm model reckons the monolayer adsorbent surface sites and homogeneous adsorption energy, while Freundlich is developed by taking account the heterogeneity of adsorbent active site. It has mathematical expression as follows

$$q_e = K_F C_e^{1/n} \quad (3)$$

where n is defined as dimensionless heterogeneity factor and K_F represents the adsorption capacity [(mmol/g)(mmol/L)$^{1/n}$]. The value of n can imply the interaction between adsorbent and adsorbate in adsorption process, it shows favorable adsorption between 1 and 10. $1/n < 1$ indicates strong interaction between adsorbent and adsorbate, while $1/n$ close to 1 signifies the homogenous adsorption energy on all active sites of adsorbent.

The azo dyes sorption at three different temperature 30 °C, 40 °C and 50 °C and fitting of Langmuir and Freundlich isotherm models is shown in Fig. 5. The isotherm parameters were calculated using non linear regression, it can be seen that Langmuir can fit experimental data better than Freundlich (Table 2). All adsorption system follows Langmuir isotherm model very well with high value of R^2, and R_L lies in between 0 and 1 which indicates the favorable adsorption of azo dyes onto NCC. Increasing temperature effects the adsorption of HB substantially, with 8.00% increase in maximum adsorption capacity from 30 °C to 50 °C. While the adsorption of CR towards NCC can give slightly higher of maximum adsorption capacity by 9.75% from 30 °C to 50 °C. This phenomena can explain that actually interaction of sorbate molecule HB is better than CR towards NCC without increasing the temperature, also adsorption of HB is higher than CR initially at all conditions (q_m HB at 30 °C = 0.1574 mmol/g, q_m CR at 30 °C = 0.1425 mmol/g). Affinity constant in adsorption of azo dyes is dependent with temperature, because K_L is related to heat of adsorption

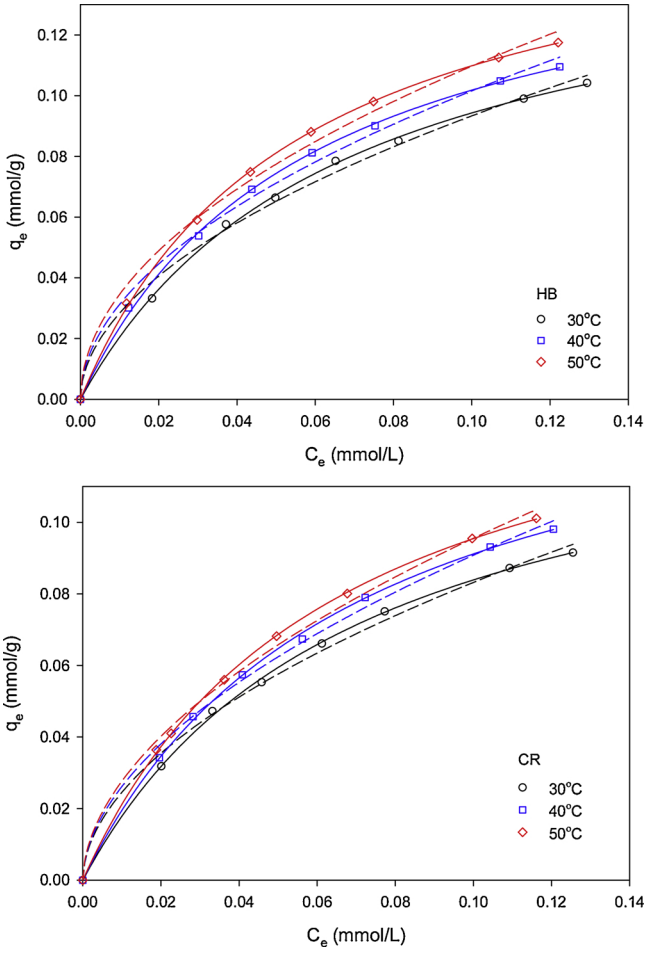

Fig. 5. Equilibrium sorption and fitting isotherm models of HB and CR dyes at 30 °C, 40 °C and 50 °C (solid line: Langmuir and dashed line: Freundlich).

Table 2
Fitting parameters of Langmuir and Freundlich isotherm models on the adsorption of HB and CR by NCC.

Azo dyes	Models	Parameters	Temperature (°C)		
			30 °C	40 °C	50 °C
HB	Langmuir	q_m(mmol/g)	0.1574	0.1612	0.1700
		K_L(L/mmol)	14.9432	17.1573	18.2749
		R_L	0.2933	0.2656	0.2534
		R^2	0.9994	0.9994	0.9997
	Freundlich	K_F(mmol/g)(mmol/L)$^{1/n}$	0.3076	0.3304	0.3486
		n	1.9314	1.9527	1.9922
		R^2	0.9933	0.9942	0.9928
CR	Langmuir	q_m(mmol/g)	0.1425	0.1541	0.1564
		K_L(L/mmol)	14.3237	14.4893	15.6503
		R_L	0.3272	0.3246	0.3080
		R^2	0.9995	0.9994	0.9998
	Freundlich	K_F(mmol/g)(mmol/L)$^{1/n}$	0.2822	0.3151	0.3299
		n	1.8859	1.8507	1.8579
		R^2	0.9953	0.9962	0.9962

in function of temperature. The higher temperature is the stronger interaction of dye molecule and NCC which point out the distinct characteristic of chemisorption mechanism. Main mechanism in this adsorption is based on the electrostatic forces of opposites charges from NCC and both dyes, which are negative and positive charges, respectively. Ionic bonding occured in the process between negative sulfonate ion of NCC and protonated functional groups from HB (hydroxyl group) and CR (ammonium or azonium group).

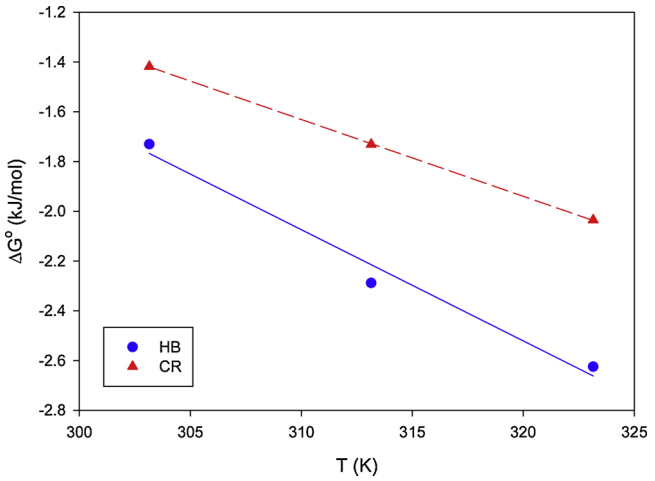

Fig. 6. Thermodynamic plot of ΔG° versus T of HB and CR adsorption on NCC.

3.5. Adsorption thermodynamics

Thermodynamic study gives information for energy and entropy occurred during the adsorption of HB and CR onto NCC. Determination of thermodynamic parameters such as Gibb's free energy (ΔG°), enthalphy (ΔH°), and entrophy (ΔS°) can be done through adsorption equilibria experimental studies with several thermodynamic equations as follow:

$$\Delta G^{o} = -RT \ln K_D \quad (4)$$

$$\Delta G^{o} = \Delta H^{o} - T\Delta S^{o} \quad (5)$$

Where R is universal gas constant (8.314 J/mol K), T is the temperature (K), and K_D is thermodynamic distribution coefficient which is an intercept obtained through linear regression of $\ln(q_e/C_e)$ versus C_e (Soetaredjo et al., 2015a, 2015b). The Gibb's free energy change can be determined using eqn. 4, and applied it on eqn. 5 versus T to obtain ΔH° and ΔS° by linear regression as intercept and slope, respectively (see Fig. 6).

Negative value of ΔG° at increasing temperature shown in Table 3 indicates favourable adsorption of both azo dyes at higher temperature. While positive value of ΔH° represent the endothermic nature of azo dyes adsorption systems, which confirms better affinity of sorbate molecule and adsorbent at higher temperature. Although both ΔH° values are not included in the range of chemisorption (20.9–418.4 kJ/mol), this standard of enthalpy is focused mainly on the chemical engineering reaction which involves the chemical reaction in reactants, whilst adsorption is particularly focus in the surface chemistry between adsorbent and adsorbate that include many types of forces such as intermolecular, electrostatic, and van der Waals forces. Small enthalpy for both azo dyes adsorption can be explained by positive and negative ions are existed in th HB and CR. Negative ions from sulfonate ion will give repulsive forces toward NCC since NCC has sulfonate functional groups. Hence protonated hydroxyl from HB and ammonium or azonium group from CR can form electrostatic forces with sulfonate ions in NCC surfaces. Positive value of ΔS° in both systems suggest that there is good affinity between sorbate molecule and adsorbent active site that causing increased randomness at solid-solution interface during adsorption.

Table 3
Thermodynamic parameters of HB and CR sorption onto NCC.

Azo dyes	Temperature (K)	ΔG° (kJ/mol)	ΔH° (kJ/mol)	ΔS° (kJ/mol K)
HB	303.15	−1.7304	11.7899	0.0447
	313.15	−2.2887		
	323.15	−2.6248		
CR	303.15	−1.4178	7.9346	0.0309
	313.15	−1.7309		
	323.15	−2.0350		

4. Conclussion

Waste printed paper can be recycled into nanocrystalline cellulose after deinking and acid hydrolysis which has yield of 30%. The adsorption of hydroxynaphtol blue and congo red on nanocrystalline cellulose has optimum adsorption at pH 2 and 3 with maximum adsorption capacity of 0.1700 mmol/g and 0.1564 mmol/g, respectively. Higher adsorption of hydroxynaphtol blue is occurred since it has more hydroxyl group in sorbate molecule compared to congo red who has transition form of ammonium and azonium. The adsorption of both azo dyes is favorable and endothermic with electrostatic forces as the main mechanism in the adsorption process.

Declaration of Competing Interest

The authors have no conflict of interest.

References

Blanchard, G., Maunaye, M., Martin, G., 1984a. Removal of heavy metals from waters by means of natural zeolites. Water Res. 18, 1501–1507. https://doi.org/10.1016/0043-1354(84)90124-6.

Crini, G., 2006a. Non-conventional low-cost adsorbents for dye removal: a review. Bioresour. Technol. 97, 1061–1085. https://doi.org/10.1016/j.biortech.2005.05.001.

Garside, P., Wyeth, P., 2006. Identification of cellulosic fibres by FTIR spectroscopy. Estud. Conserv. E Restauro 51, 205–211. https://doi.org/10.1179/sic.2006.51.3.205.

Gupta, V.K., Suhas, 2009a. Application of low-cost adsorbents for dye removal - a review. J. Environ. Manage. 90, 2313–2342. https://doi.org/10.1016/j.jenvman.2008.11.017.

He, X.Y., Male, K.B., Nesterenko, P.N., Brabazon, D., Paull, B., Luong, J.H.T., 2013a. Adsorption and Desorption of Methylene Blue on Porous Carbon Monoliths and Nanocrystalline Cellulose Adsorption and Desorption of Methylene Blue on Porous Carbon Monoliths and Nanocrystalline Cellulose. https://doi.org/10.1021/am403222u.

Higgins, H.G., Stewart, C.M., Harrington, K.J., 1961a. Infrared spectra of cellulose and related polysaccharides. J. Polym. Sci. 51, 59–84. https://doi.org/10.1002/pol.1961.120510105.

Ioelovich, M., 2008a. Cellulose as a nanostructured polymer: a short review. BioResources 3, 1403–1418. https://doi.org/10.15376/biores.3.4.1403-1418.

Itoh, B.Y.A., Ueno, K., 1970a. as Metallochromic Indicators in the EDTA Titration of Calcium 95. pp. 583–589.

Jin, L., Sun, Q., Xu, Q., Xu, Y., 2015a. Adsorptive removal of anionic dyes from aqueous solutions using microgel based on nanocellulose and polyvinylamine. Bioresour. Technol. 197, 348–355. https://doi.org/10.1016/j.biortech.2015.08.093.

Kant, R., 2012a. Textile dyeing and printing industry: an environmental hazard. Nat. Sci. (Irvine) 4, 22–26. https://doi.org/10.4236/ns.2012.41004.

Lagergren, S., 1898a. About the theory of so-called adsorption of soluble substance. K. Sven. Vetenskapsakademiens Handl. 24, 1–39.

Lee, J., Kim, S.H., Cho, Y.J., Nam, Y.S., Lee, K.B., Lee, Y., 2014a. Characterization and sequence determination of pen inks, red sealing inks, and laser toners by TOF-SIMS and ATR FTIR. Surf. Interface Anal. 46, 317–321. https://doi.org/10.1002/sia.5535.

Lin, N., Dufresne, A., 2014a. Surface chemistry, morphological analysis and properties of cellulose nanocrystals with gradiented sulfation degrees. Nanoscale 6, 5384–5393. https://doi.org/10.1039/C3NR06761K.

McKay, R., Hillson, P., 1965a. Metachromatic behaviour of dyes in solution. Trans. Faraday Soc. 61, 1800–1810.

Mera, S.L., Davies, J.D., 1984a. Differential Congo Red staining: the effects of pH, non-aqueous solvents and the substrate. Histochem. J. 16, 195–210. https://doi.org/10.1007/BF01003549.

Merrill, R.A., Bartick, E.G., Taylor, J.H., 2003a. Forensic discrimination of photocopy and printer toners I. The development of an infrared spectral library. Anal. Bioanal. Chem. 376, 1272–1278. https://doi.org/10.1007/s00216-003-2073-0.

Pigorsch, E., Elhaddaoui, A., Turrell, S., 1994a. Spectroscopic study of pH and solvent effects on the structure of Congo red and its binding mechanism to amyloid-like proteins. Spectrochim. Acta Part A Mol. Spectrosc. 50, 2145–2152. https://doi.org/10.1016/0584-8539(94)00151-0.

Qiao, H., Zhou, Y., Yu, F., Wang, E., Min, Y., Huang, Q., Pang, L., Ma, T., 2015a. Effective removal of cationic dyes using carboxylate-functionalized cellulose nanocrystals. Chemosphere 141, 297–303. https://doi.org/10.1016/j.chemosphere.2015.07.078.

Research Conservation Alliance, 2016. Focus on Paper Consumption. URL www.woodconsumption.org (Accessed 12.15.16). .

Sabnis, R.W., 2010a. Handbook of Biological Dyes and Stains: Synthesis and Industrial Applications. John Wiley & Sons, Inc., United Stated of America. https://doi.org/10.1002/9780470586242.

Soetaredjo, F.E., Ismadji, S., Ayucitra, A., Ju, Y.-H., 2015a. In: Yu, F. (Ed.), Recent Advances in the Application of Polymer - Based Nanocomposites for Removal of Hazardous Substances from Water and Wastewater. Scrivener Publishing LLC.

Yu, X., Tong, S., Ge, M., Wu, L., Zuo, J., Cao, C., Song, W., 2013a. Adsorption of heavy metal ions from aqueous solution by carboxylated cellulose nanocrystals. J. Environ. Sci. (China) 25, 933–943. https://doi.org/10.1016/S1001-0742(12)60145-4.

Blanchard, G., Maunaye, M., Martin, G., 1984b. Removal of heavy metals from waters by means of natural zeolites. Water Res. 18 (2), 1501–1507.

Crini, G., 2006b. Non-conventional low-cost adsorbents for dye removal: a review. Bioresour. Technol. 97 (9), 1061–1085.

Gupta, V.K., Suhas, 2009b. Application of low-cost adsorbents for dye removal – a review. J. Environ. Manage. 90, 2313–2342.

He, X., Male, K.B., Nesterenko, P.N., Brabazon, D., Paull, B., Luong, J.H.T., 2013b. Adsorption and desorption of methylene blue on porous carbon monoliths and nanocrystalline cellulose. ACS Appl. Mater. Interfaces 5, 8796–8804.

Higgins, H.G., Stewart, C.M., Harrington, K.J., 1961b. Infrared spectra of cellulose and related polysaccharides. J. Polym. Sci. 51, 59–84.

Ioelovich, M., 2008b. Cellulose as a nanostructured polymer: a short review. BioResources 3 (4), 1403–1418.

Itoh, A., Ueno, K., 1970b. 2-Hydroxy-1-(2-hydroxy-4-sulpho-1-napthylazo)-3-naphthoic acid and hydroxynaphtol blue as metallochromic indicators in the EDTA titration of calcium. Analyst 95, 583–589.

Jin, L., Sun, Q., Xu, Q., Xu, Y., 2015b. Adsorptive removal of anionic dyes from aqueous solutions using microgel based on nanocellulose and polyvinilamine. Bioresour. Technol. 197, 348–355.

Kant, R., 2012b. Textile dyeing industry an environmental hazard. Nat. Sci. (Irvine) 4 (1), 22–26.

Lagergren, S., 1898b. Zur theorie der sogenannten adsorption gelöster stoffe. Kunglinga Svenska Vetenskapsademiens. Handlingar 24 (4), 1–39.

Lee, J., Kim, S.H., Cho, Y.J., Nam, Y.S., Lee, K.B., Lee, Y., 2014b. Characterization and sequence determination of pen inks, read sealing inks, and laser toners by TOF-SIMS and ATR FTIR. Surf. Interface Anal. 46, 317–321.

Lin, N., Dufresne, A., 2014b. Surface chemistry, morphological analysis and properties of cellulose nanocrystals with gradiented sulfation degrees. Nanoscale 6, 5384–5392.

McKay, R.B., Hillson, P.J., 1965b. Metachromatic behaviour of dyes in solution. Interpretation on the basis of interaction between dye ions and counter ions. Trans. Faraday Soc. 61, 1800–1810.

Mera, S.L., Davies, J.D., 1984b. Differential congo red staining: the effects of pH, non-aqueous solvents and the substrate. Histochem. J. 16, 195–210.

Merrill, R.A., Bartick, E.G., Taylor III, J.H., 2003b. Forensic discrimination of photocopy and printer toners. I. The development of an infrared spectral library. Anal. Bioanal. Chem. 376, 1272–1278.

Pigorsch, E., Elhaddaoui, A., Turrell, S., 1994b. Spectroscopic study of pH and solvent effects on the structure of congo red and its binding mechanism to amyloid-like proteins. Spectrochim. Acta 50A, 2145–2152.

Qiao, H., Zhou, Y., Yu, F., Wang, E., Min, Y., Huang, Q., Pang, L., Ma, T., 2015b. Effective removal of cationic dyes using carboxylate-functionalized cellulose nanocrystals. Chemosphere 141, 297–303.

Sabnis, R.W., 2010b. Handbook of Biological Dyes and Stains. Synthesis and Industrial Applications. John Wiley & Sons, Canada.

Soetaredjo, F.E., Ismadji, S., Ayucitra, A., Ju, Y.H., 2015b. In: Yu, F. (Ed.), Recent Advances in the Application of Polymer-Based Nanocomposites for Removal of Hazardous Substances from Water and Wastewater.

Yu, X., Tong, S., Ge, M., Wu, L., Zuo, J., Cao, C., Song, W., 2013b. Adsorption of heavy metal ions from aqueous solution by carboxylated cellulose nanocrystals. J. Environ. Sci. 25 (5), 933–943.